Clinical Neurology and Neurosurgery 241 (2024) 108305

Contents lists available at ScienceDirect

Clinical Neurology and Neurosurgery

journal homepage: www.elsevier.com/locate/clineuro

Differential tractography and whole brain connectometry in primary motor area gliomas resection: A feasibility study

Luisa F. Figueredo [a], Juan A. Mejía-Cordovez [b], Diego A. Gomez-Amarillo [b], Fernando Hakim [b], Hebert D. Pimienta-Redondo [c], Joao P. Almeida [d], Ivo Kehayov [e], Polina Angelova [e], Georgi Apostolov [e], Sabino Luzzi [f,g], Matías Baldoncini [h,i], Jason M. Johnson [j], Edgar G. Ordóñez-Rubiano [b,c,k,*]

[a] Healthy Brain Aging and Sleep Center (HBASC), Department of Psychiatry at NYU Langone School of Medicine, New York, NY, United States
[b] Department of Neurosurgery, Fundación Santa Fe de Bogotá, Bogotá, Colombia
[c] Department of Neurosurgery, Hospital de San José, Fundación Universitaria de Ciencias de la Salud, Bogotá, Colombia
[d] Department of Neurosurgery, Mayo Clinic Florida, Jacksonville, FL, United States
[e] Department of Neurosurgery, Medical University of Plovdiv, Plovdiv, Bulgaria
[f] Neurosurgery Unit, Department of Surgical Sciences, Fondazione IRCCS Policlinico San Matteo, Pavia, Italy
[g] Neurosurgery Unit, Fondazione IRCCS Policlinico San Matteo, Pavia, Italy
[h] School of Medicine, Laboratory of Microsurgical Neuroanatomy, Second Chair of Gross Anatomy, Buenos Aires, Argentina
[i] Department of Neurological Surgery, Hospital San Fernando, Buenos Aires, Argentina
[j] Department of Radiology, MD Anderson, The University of Texas, Houston, TX, United States
[k] School of Medicine, Universidad Nacional de Colombia, Bogotá, Colombia

ARTICLE INFO

Keywords:
Glioma
tractography
connectome
connectometrics
connectomics

ABSTRACT

Objective: Establish the evolution of the connectome before and after resection of motor area glioma using a comparison of connectome maps and high-definition differential tractography (DifT).
Methods: DifT was done using normalized quantitative anisotropy (NQA) with DSI Studio. The quantitative analysis involved obtaining mean NQA and fractional anisotropy (FA) values for the disrupted pathways tracing the corticospinal tract (CST), and white fiber network changes over time.
Results: We described the baseline tractography, DifT, and white matter network changes from two patients who underwent resection of an oligodendroglioma (Case 1) and an IDH mutant astrocytoma, grade 4 (Case 2). Case 1. There was a slight decrease in the diffusion signal of the compromised CST in the immediate postop. The NQA and FA values increased at the 1-year follow-up (0.18 vs. 0.32 and 0.35 vs. 0.44, respectively). Case 2. There was an important decrease in the immediate postop, followed by an increase in the follow-up. In the 1-year follow-up, the patient presented with radiation necrosis and tumor recurrence, increasing NQA from 0.18 in the preop to 0.29. Fiber network analysis: whole-brain connectome comparison demonstrated no significant changes in the immediate postop. However, in the 1-year follow up there was a notorious reorganization of the fibers in both cases, showing the decreased density of connections.
Conclusions: Connectome studies and DifT constitute new potential tools to predict early reorganization changes in a patient's networks, showing the brain plasticity capacity, and helping to establish timelines for the progression of the tumor and treatment-induced changes.

Abbreviations: CST, corticospinal tract; DifT, differential tractography; DSS, direct subcortical stimulation; DTI, diffusion tensor imaging; DTT, diffusion tensor tractography; EOR, extent of resection; FA, fractional anisotropy; FMRI, functional magnetic resonance imaging; KPS, Karnofsky Performance Scale; NQA, normalized quantitative anisotropy; QA, quantitative anisotropy.

* Correspondence to: Department of Neurosurgery, Hospital de San José, Fundación Universitaria de Ciencias de la Salud, Calle 10# 18-75, Columbia.
E-mail address: egordonez@fucsalud.edu.co (E.G. Ordóñez-Rubiano).

https://doi.org/10.1016/j.clineuro.2024.108305
Received 11 March 2024; Accepted 24 April 2024
Available online 25 April 2024

1. Introduction

Park and Friston assert that the human brain poses a complex paradox, suggesting that its resolution could lie in the brain's network structure, which manages interactions essential for various requirements, enabling flexibility despite static anatomy [1]. This underscores the reliance of our comprehension of brain connectivity on measurement and modeling methods, emphasizing the need for a systematic computational approach to elucidate the relationship between structure and function. Furthermore, it emphasizes how the brain dynamically reorganizes in response to internal and external stimuli. Notably, one of the most significant challenges could be tumor growth and the ensuing medical interventions.

Gliomas originate from neuroglial stem or progenitor cells within the brain [2]. The standard approach for glioma resection involves brain mapping techniques such as intraoperative neurophysiology and neuropsychology [3]. Additionally, modern intraoperative neuroimaging methods are increasingly utilized to safeguard vital brain regions and enhance post-surgical results. Especially, tractography is commonly employed both before and during surgery, especially when dealing with tumors near critical areas [4–10]. It offers insights into how tumors impact white matter tracts and can be used quantitatively for preoperative brain mapping, assessing postoperative fiber integrity, and analyzing data obtained from intraoperative direct subcortical stimulation (DSS) [11,12].

Differential tractography (DifT) offers a method to analyze repeat scans of an individual, aiming to detect alterations in fiber pathways by observing changes in fractional anisotropy (FA) through a *"tracking the difference"* approach [4]. Additionally, DifT compares preoperative changes with a reference database of healthy individuals to identify disrupted white matter pathways that may not typically undergo preoperative evaluation or prove difficult to assess otherwise [4]. The goal of this study is to employ DifT in assessing immediate and short-term alterations in connectomics following primary motor area (M1) glioma resection. Additionally, the study aims to conduct a comparative examination of the entire connectome between preoperative and successive postoperative scans to assess neural reorganization and its correlation with clinical results.

2. Methods

The study comprised two adult patients who underwent surgical resection of M1 gliomas. Data analysis was conducted with one reviewer (L.F.) blinded to the patient's clinical characteristics. Tumor resection was performed by the senior author (E.O.) in both cases. Approval for the study was obtained from the local Institutional Review Board and Ethics Board, and informed consent was obtained from each patient. The research was conducted following the principles outlined in the Declaration of Helsinki.

2.1. Diffusion weighted imaging (DWI) data acquisition and processing

The diffusion images were obtained using a Siemens MAGNETOM® Aera (1.5 T Siemens Healthcare, Erlangen, Germany) scanner employing a 2D EPI diffusion sequence. Parameters included TE=86 ms and TR=2800 ms. A HARDI scheme was employed with 128 diffusion sampling directions, and the b-value was set at 1000 s/mm^2. The in-plane resolution was 1.30682 mm with a slice thickness of 6.5 mm. The diffusion MRI data were resampled to achieve a 2 mm isotropic resolution. The DSI Studio software (http://dsi-studio.labsolver.org) was utilized to visualize the entire brain and the corticospinal tract (CST) employing a generalized deterministic tractography method with the DSI datasets. To mitigate the potential for false outcomes, we ensured consistency in image dimensions, resolution, and b-table between repeated scans. Additionally, a slice-wise quality assessment was conducted for each diffusion-weighted image. Data with a dropout slice number less than 0.1% were deemed acceptable. A comprehensive whole-brain seeding approach was employed to validate the quality of the reading. The threshold, as provided standard by DSI Studio, remained consistent across longitudinal scans but was adjusted and augmented specifically for the DifT analysis.

2.1.1. Fiber tracking

Fiber tracking was initiated by employing random orientations within a voxel until 50,000 streamlines were detected. The following parameters were utilized: a maximum turning angle of 90 degrees, a smoothing factor of 0.8, and a length constraint ranging from 150 to 200. A HARDI scheme was adopted with 128 diffusion sampling directions and a b-value of 1000 s/mm^2. The in-plane resolution was 1.30682 mm, and the slice thickness was 6.5 mm. The diffusion MRI data were resampled to achieve a 2 mm isotropic resolution. To investigate neuronal changes, the diffusion data were compared with a baseline scan using DifT with a diffusion sampling length ratio of 1.25. An automated seeding region was placed along the hand knob in the CST bilaterally. The region of interest (ROI) was positioned within the track tolerance region with a volume of 1.1e+06 mm^3. The anisotropy threshold and angular threshold were randomly selected within ranges of values. The step size was randomly chosen between 0.5 and 1.5 voxels. Tracks with lengths shorter than 30 mm or longer than 300 mm were discarded, and a total of 500,000 seeds were placed for tracking.

2.1.2. Differential tractography technique

Restricted and increased diffusion were quantified, and the diffusion data were compared with a baseline scan using DifT with a diffusion sampling length ratio of 1.25 to analyze neuronal changes. DifT was utilized to map pathways exhibiting an increase or decrease in quantitative anisotropy, with only differences exceeding 20% being tracked. A seeding region encompassing the entire brain was designated, with the anisotropy threshold and angular threshold being randomly selected within specified ranges. The step size was randomly chosen between 0.5 and 1.5 voxels. Tracks with lengths shorter than 30 mm or longer than 300 mm were excluded and a total of 500,000 seeds were generated for tracking. A threshold of 45–75% was maintained, and topology-informed pruning was employed with 16 iterations to eliminate false connections in the tractography.

2.1.3. Differential whole brain connectometry technique

A whole-brain connectome analysis was conducted for each case using data from the Human Connectome Project (HCP) Database [13]. Graph theory measures were extracted to assess changes between MRI scans utilizing DSI Studio software, with the "FIB.gz" files extracted for each patient and scan. Whole-brain fiber tracking was performed for each scan using 10,000,000 seeds. Subsequently, a connectivity matrix was generated employing the HCP842_tractography atlas [14]. A threshold of 50% was applied to create a whole-brain connectome, which was saved as a matrix of dimensions 15 ×15 in.txt format. This file was utilized to generate a connectogram using the CIRCOS software package (http://mkweb.bcgsc.ca/tableviewer/visualize/). The graph was constructed based on quartiles and color-coded for ease of interpretation: Q1 interactions, representing the strongest interactions in the analysis, were depicted in light blue, Q2 interactions in green, Q3 in light gray, and Q4 in dark grey.

3. Results

3.1. Case #1

3.1.1. Grade II oligodendroglioma

A 38-year-old male presented with focal seizures and a left upper limb hemiparesis graded at 4/5. Upon admission, his initial Karnofsky Performance Scale (KPS) score was 90/100. MRI revealed an M1 glioma with minimal enhancement in T1 post-gadolinium administration

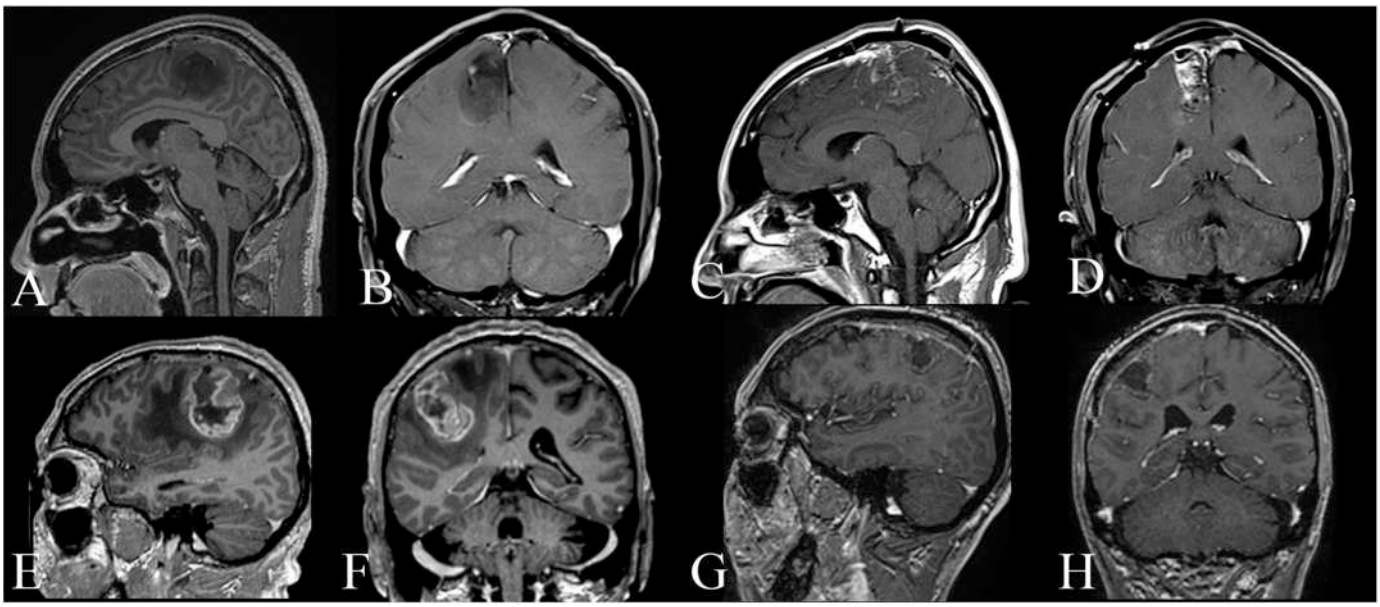

Fig. 1. Pre- and postoperative MRI scans. *Case #1.* (A, B) Preop MRI demonstrates an intra- axial M1 tumor with minimal enhancement after gadolinium administration. (C, D) Immediate postoperative sagittal and axial images show a near-total resection. *Case #2.* (E, F) Preop MRI shows a right intra-axial M1 tumor, with heterogeneous enhancement after contrast administration and significant perilesional edema. (G, H) The 1-year follow-up MRI following adjuvant chemotherapy and radiotherapy demonstrated satisfactory tumor control.

(Fig. 1). Preoperative tractography displayed anteromedial displacement of the CST (Fig. 2). Surgical resection guided by direct DSS using CST tractography as a navigation tool resulted in a radiologically safe near-total resection, consistent with intraoperative findings. Immediate postoperative tractography indicated the expected preservation of the CST following DSS guidance. Histological analysis revealed an oligodendroglioma WHO grade II based on molecular and immunochemistry results. The patient experienced no postoperative neurological deterioration. At the 1-year follow-up, he retained a 4/5 left hemiparesis but maintained ambulation and independence in daily activities.

3.1.2. Case #2

3.1.2.1. IDH mutant grade IV astrocytoma. A 54-year-old man initially experienced focal seizures in his left upper limb, which subsequently generalized, leading to loss of consciousness lasting at least five minutes, followed by hemiparesis (3/5 in the left arm and 4/5 in the left leg). MRI revealed a large M1 enhancing tumor (Fig. 1). Upon admission for surgery, his preoperative KPS score was 70/100. Surgical resection was performed utilizing both preoperative diffusion tensor imaging and intraoperative stimulation techniques. Histopathological, immunochemistry and molecular analyses confirmed the diagnosis of an IDH-mutant astrocytoma, grade IV, according to the WHO 2021 classification [15]. Postoperatively, the hemiparesis improved, suggestive of Todd's paralysis and effective decompression of motor pathways. The patient was initiated on the conventional STUPP protocol. The 1-year postoperative MRI revealed tumor progression with diffuse involvement of the CST. Because the risk outweighed the benefit of reintervention, complementary treatment with Bevacizumab at a dosage of 640 mg was administered intravenously over three doses, typically given every 2 or 3 weeks. In the 18-month follow-up, the patient exhibited upper left limb monoparesis rated at 3/5, and continued to necessitate anticonvulsants to manage refractory epilepsy.

3.1.3. Differential tractography data

In case #1, the preoperative tractography revealed a subtle rearrangement of the right CST and an intact left CST (Fig. 3). Upon immediate postoperative evaluation, there was a decrease in normalized quantitative anisotropy (NQA) for both CST tracts, although the fibers remained intact. However, in the 1-year follow-up, there appeared to be evidence of recovery in fiber volumes.

In contrast, in case #2, the preoperative tractography showed no direct compromise of the CST by the tumor core but rather by the tumor margin and peritumoral edema (Fig. 3). The immediate postoperative image exhibited a subtle re-arrangement of fibers around the resection area, resembling the contralateral CST. However, the 1-year postoperative image revealed a disorganized distribution of fibers, with decreased NQA observed in the right CST compared to the left.

In terms of volume, both cases exhibited a transient increase in tract volume immediately postoperatively, which returned close to baseline levels in the follow-up scans. However, in case #2, the decrease in volume was more pronounced. Interestingly, the contralateral CST showed an increase in volume in the 1-year follow-up, suggesting contralateral neural reorganization.

Quantitatively, in case #1, the preoperative volume of the right CST was 3226 mm^3, increasing substantially immediately postoperatively, likely due to decompression, and subsequently decreasing to 3171 mm^3 in the follow-up (Table 1). The NQA also changed in case #1 in the 1-year follow-up, increasing nearly double from the initial value (0.18–0.32). FA remained similar, with a slight increase in the follow-up (0.35–0.44) (Fig. 4).

For case #2, changes in the volume of the right CST tract were more pronounced. The initial volume was 2301 mm^3, increasing significantly to 9819 mm^3 immediately postoperatively, and then decreasing to 1365 mm^3 in the 1-year postoperative scan. In terms of NQA, case #2 exhibited different changes in morphology, with an initial value of 0.18 preoperatively and a non-statistically significant increase to 0.29 postoperatively. No further changes were observed in FA.

For case #1, most comparisons between preoperative tractography and immediate postoperative scans did not reveal significant differences (Fig. 5). However, some nonspecific changes were observed when comparing immediate postoperative with 1-year follow-up scans. The final comparison for case #1, between preoperative and 1-year follow-up scans, demonstrated a decrease primarily in the perilesional area without affecting the right CST.

In contrast, for case #2, no notable changes were observed when

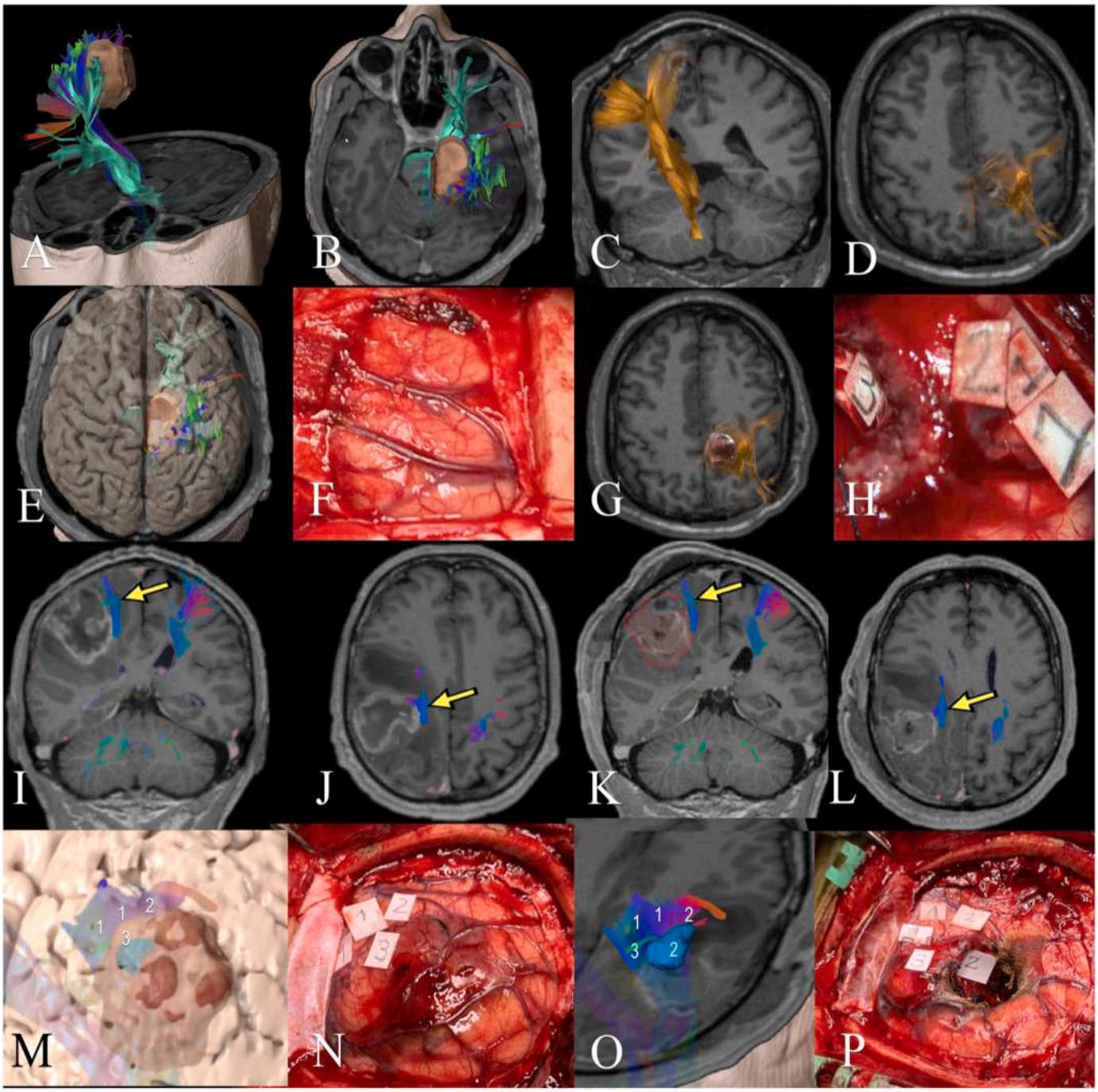

Fig. 2. Pre- and postoperative tractography and intraoperative images of brain mapping. *Case #1*: (A, B) Preoperative tractography demonstrates lateral displacement of the right CST. The rest of the anterior corona radiata is represented in green. (C, D) Postoperative tractography shows the preservation of the CST with partial recovery of its anatomical location. (E) Volumetric reconstruction of the brain surface, the tumor, and CST are shown. (F) Intraoperative imaging of the cortex is demonstrated, showing no superficial cortical abnormalities. (G) Postoperative tractography shows a 3D reconstruction of the resection cavity associated with the preserved CST. (H) The intraoperative picture shows the preservation of the areas corresponding to the left upper limb (1, 2, 3), delineating the resection boundaries. *Case #2:* (I, J) Preoperative tractography demonstrates a CST medial displacement (arrow). (K, L) Postoperative T1 postcontrast images show preservation of the CST. (M, O) 3D reconstructions illustrate postoperative patency of the CST in close relationship with a medial residual in the most superficial aspect of the resection cavity, which is depicted in blue. (M, O) Comparative fused images of pre-and postoperative tractography show the intimal relationship of the CST, numbered by the function of the thumb (1), the shoulder (2), and the hand (3). The blue residual was marked as eloquent during the stimulation. The areas of the thumb (1), shoulder (2), and hand (3) are shown in the intraoperative pictures before (N) and after (P) resection.

comparing preoperative tractography with immediate postoperative scans or between immediate postoperative and 1-year follow-up scans. However, when comparing 1-year follow-up scans with preoperative scans, a marked decrease was observed, particularly associated with the right CST.

3.1.4. Whole brain connectometry data

In the comparison of DifT results from case #2 with the HCP control connectometry group, no significant differences or direct compromise of the CST by the tumor were observed. However, there was discreet displacement of the tract in the perilesional area. Notably, there was no

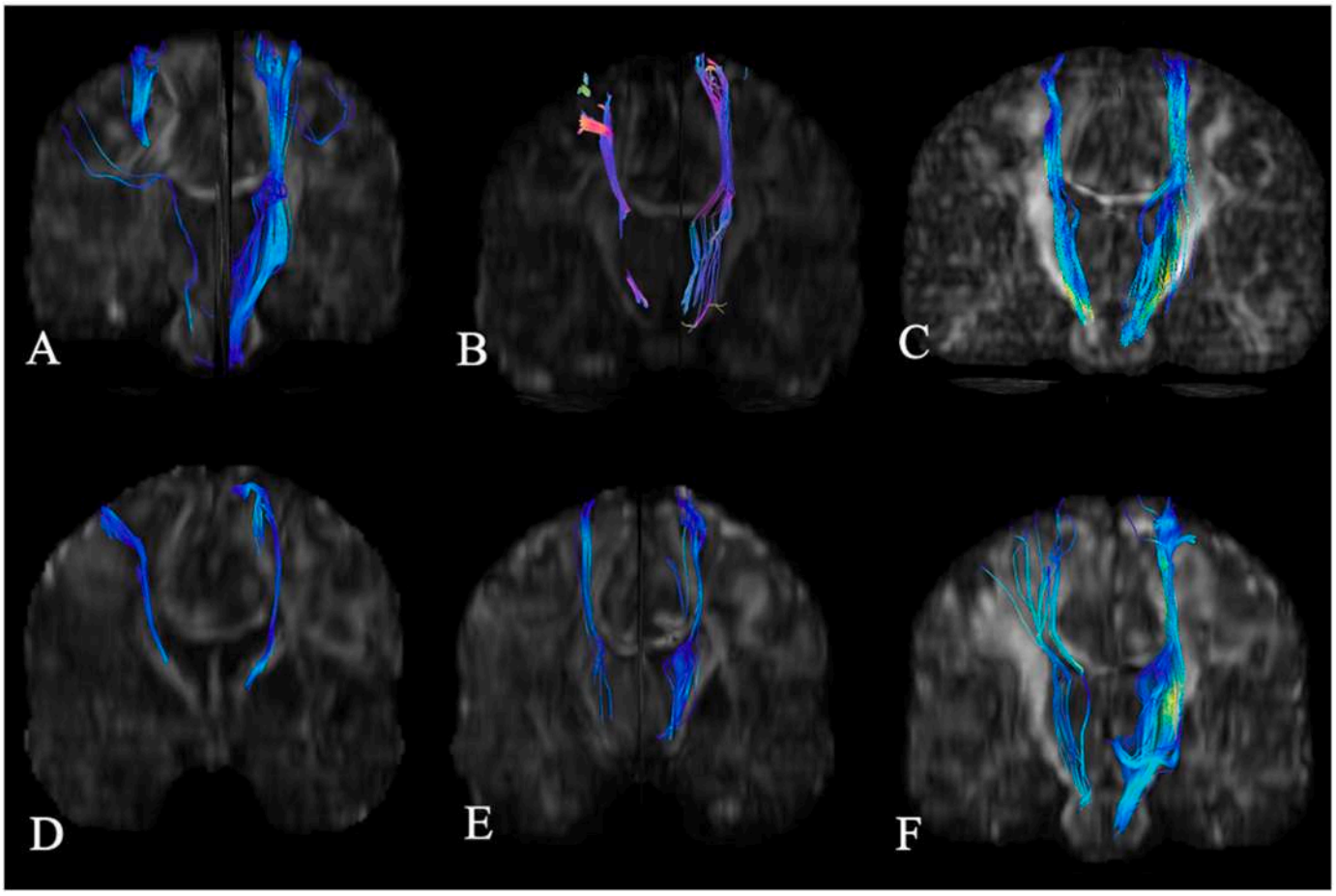

Fig. 3. CST tractography. *Case #1.* (A) Preoperative tractography demonstrates a subtle reorganization of the CST in the right and an intact left CST. (B) Immediate postoperative tractography shows a decrease in the NQA for both CST tracts without complete disruption of the fibers. (C) 1-year follow-up tractography demonstrates a recovered distribution and volume of the fibers on both sides. *Case #2.* (D) Preoperative tractography demonstrates a compromised NQA in the right CST and the fibers surrounding the margin of the tumor. (E) Immediate postoperative tractography shows a mild reorganization of the right CST, where some lateral fibers wrapping the tumor are now absent. (F) One-year follow-up images demonstrate increased NQA in both CST. The right CST shows a re-establishment of the fibers in the previous tumoral area; however, the tract appears to have less volume, possibly associated with displacement of the fibers, recurrence, and radiation therapy.

Table 1
Corticospinal tract quantitative anisotropy values.

	Tract	Laterality	Volume (mm^3)	Diameter (mm)	QA	NQA	FA
Case 1	Corticospinal Tract Pre-OP	Left	4641	6.331	0.886	0.19	0.396
		Right	3236	5.391	0.836	0.18	0.356
	Corticospinal Tract Post Op (Immediate)	Left	5230	6.71	0.866	0.11	0.345
		Right	7287	8.48	0.77	0.1	0.325
	Corticospinal Tract Post Op	Left	3730	5.86	1.2	0.29	0.417
	(1 Year)	Right	3171	5.67	1.3	0.32	0.44
Case 2	Corticospinal Tract Pre-OP	Left	2464	4.91	0.8	0.18	0.39
		Right	2301	4.62	0.77	0.18	0.3
	Corticospinal Tract Post Op (Immediate)	Left	5252	6.75	0.86	0.17	0.36
		Right	9819	9.67	0.8	0.16	0.3
	Corticospinal Tract Post Op	Left	8539	8.6	0.96	0.28	0.36
	(1 Year)	Right	1365	2.21	1	0.29	0.38

QA: quantitative anisotropy; NQA: normalized quantitative anisotropy;FA: fractional anisotropy

evident decrease in diffusion, suggesting edematous compromise rather than direct infiltration or disruption of fibers (Fig. 6). This finding underscores the nuanced nature of the tumor's impact on surrounding brain structures and highlights the importance of utilizing comprehensive datasets like the HCP database for comparative analysis.

In the connectogram presented in Fig. 7, a whole-brain network tracking the white matter tracts was performed. In the baseline preoperative connectogram of case #1, there was a stronger association between the left-sided tracts. Immediately postoperatively, there was an increase in connections bilaterally. At the 1-year follow-up, there was a stronger association of the left tracts, with a slight decrease observed on the right.

For case #2, the baseline connectogram exhibited heterogeneous strength and structure between the tracts, with a slight preference for the left. The immediate postoperative scan showed a similar increased distribution of connections. However, at the 1-year follow-up, fewer

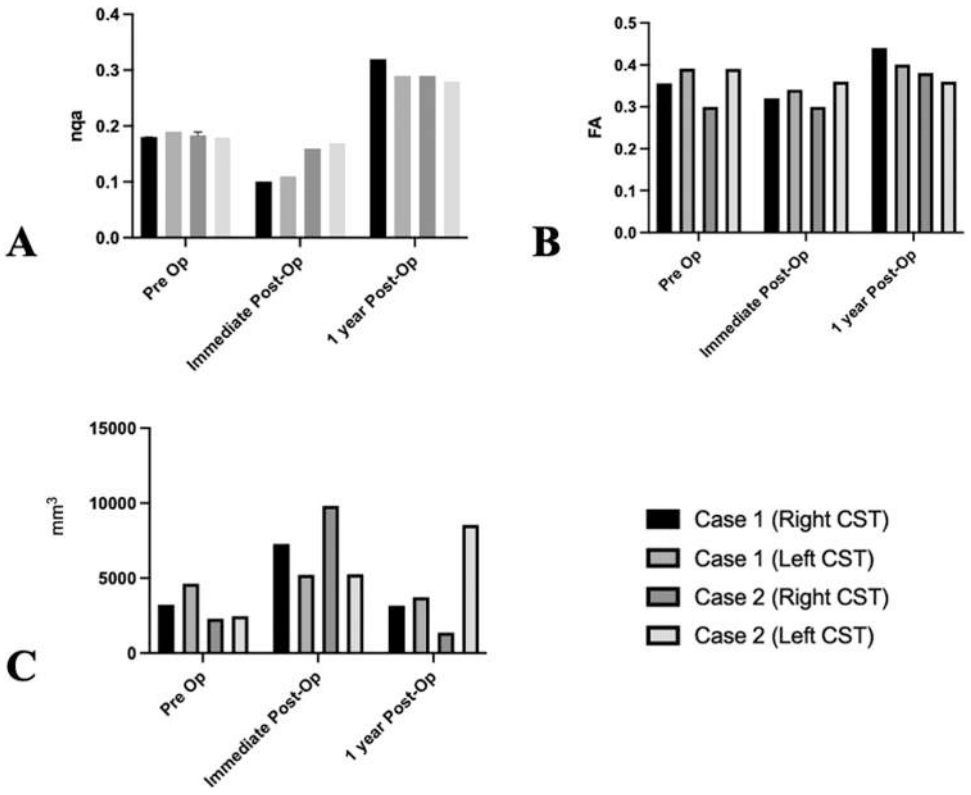

Fig. 4. (A) Changes in the NQA in the different time points comparing the CST bilaterally. No statistically significant changes were found. (B) Changes in FA values are shown. No statistically significant differences were noted. (C) Changes in the CST volume in the different time points comparing the CST bilaterally are illustrated. The only statistically significant result corresponded to the volume of case #2 in the right CST in the immediate postoperative tractography compared to a one-year follow-up (<0.0001).

connections were observed, primarily in terms of strength, with no presence noted on the right side.

4. Discussion

Here, we present the application of two neuroimaging techniques to demonstrate immediate postoperative and 1-year follow-up changes in fiber tracts of glioma patients. Our findings support the early postoperative viability of the CST through a robust quantitative analysis of the tracts, comparing diffusion data to standard available databases. In the context of this study, DifT operates on the principle of *"tracking the differences"* focusing on identifying decreases in function.

DifT enables a comprehensive examination, comparing different time points within the same patient to elucidate how the tracts are affected by tumor, edema, or surgery, thereby facilitating more accurate radiological follow-up and recovery prognosis. In contrast, whole-brain connectometry reveals the lateralization and strength of association between white fiber tracts, with some of these associations decreasing in more aggressive treatments or recurrence scenarios. Additionally, it quantitatively assesses the clinical status of motor function, thereby reinforcing its anatomical and functional integrity.

Advanced imaging methods play a crucial role in assessing the degree of fiber reorganization [16–19]. Specifically, tractography data aids in reconstructing a three-dimensional map of the tract, which represents functional networking involving aspects such as tumor localization, surgical planning, patient positioning, and flap design. However, traditional tractography alone may not always ascertain whether the tract is functional or predicts postoperative changes, such as increases or decreases in function.

Integrative functions, such as comparing quantitative anisotropy and FA, offer additional data and valuable insights for predicting functional outcomes. By analyzing QA and FA concurrently, clinicians can gain a deeper understanding of the structural and functional integrity of white matter tracts, enhancing their ability to anticipate postoperative or posttraumatic changes in neurological function [20,21]. In our study, we assessed the EOR and any tract disruption. Figs. 2 and 3 demonstrated adequate resection with preservation of the CST. In case #1, DifT revealed a decrease in diffusion in the ipsilateral temporal lobe, partially corresponding to the right CST (Fig. 6). However, this decrease did not extend to the resection area, suggesting modification of the tract due to tissue manipulation rather than direct tumor resection. This finding could potentially be a false positive or indicative of certain areas' sensitivity to the surgical procedure, as noted by Yeh et al. [4]. Quantitative analysis of the CST showed an increase in NQA on the right side, where the lesion was located, supporting functional preservation. FA did not exhibit significant changes, which may be attributed to the impact of edema on tract volume [22,23]. In case #2, postoperative tractography demonstrated adequate preservation of the tract immediately postoperatively, despite distorted anatomy. However, in the follow-up, we observed displacement and disruption of fibers, with a significant reduction in the right CST volume compared to the immediate postoperative scan, indicative of tumor progression.

Quantitatively, the NQA for the right CST remained consistent compared to preoperative tractography in the 1-year follow-up (0.3–0.38), potentially related to partial preservation of motor function. However, initial structural changes may precede functional deficits, as the tumor initially impacts tract volume. This information is crucial for understanding tumor progression and its impact on CST integrity and function. At this stage, diffuse tumor involvement affects not only the CST but also whole-brain connectivity compared to the immediate postoperative state. This information must be complemented with data obtained from connectometry to provide a comprehensive understanding of tumor progression and its effects on brain connectivity.

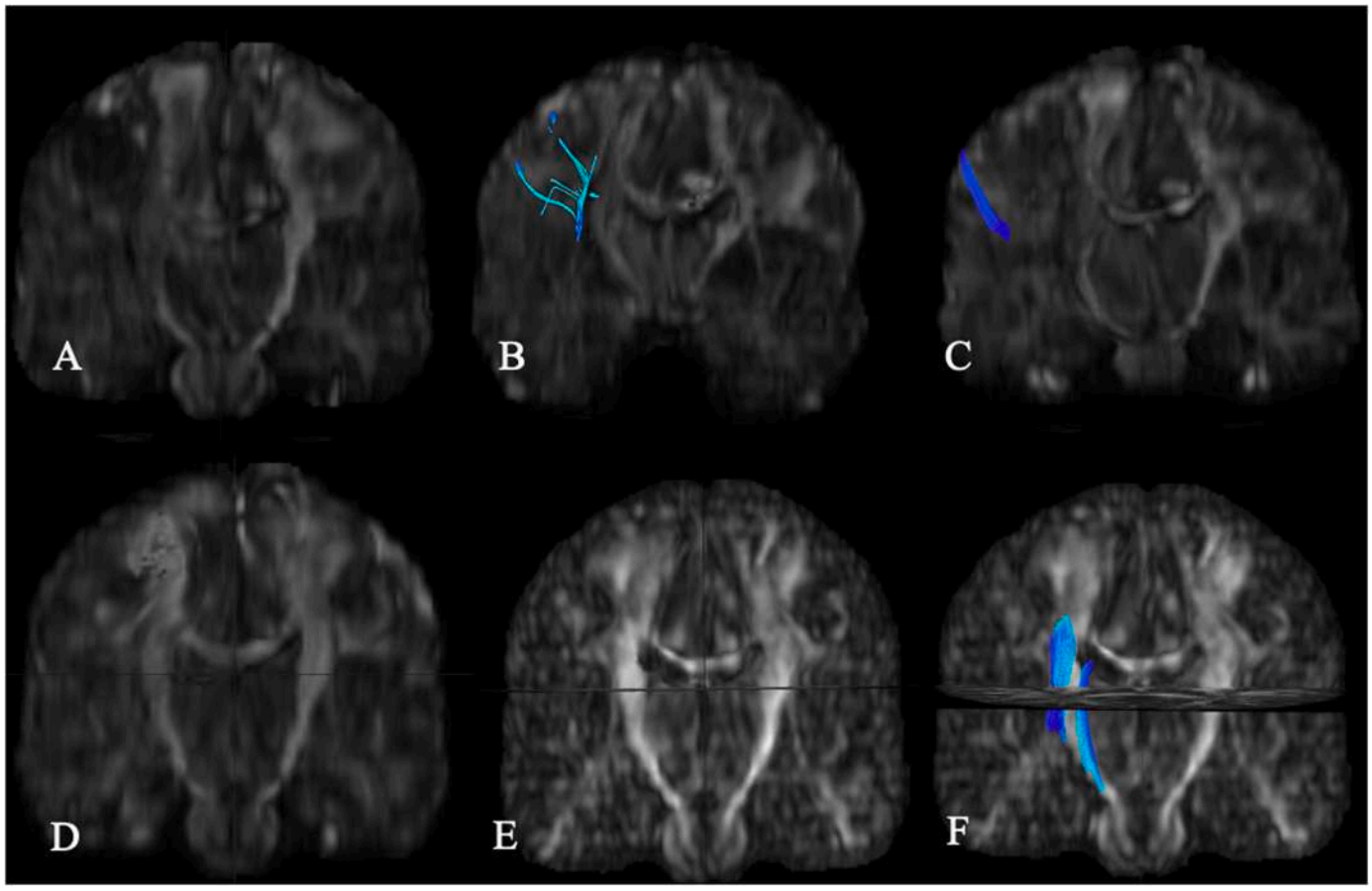

Fig. 5. Differential Tractography. (A) *Case #1*. Preoperative tractography vs. immediate postoperative tractography evaluating changes in the NQA. This differential tractography demonstrates no changes in the CSTs between both scans. (B) Immediate postop tractography vs. one-year follow-up tractography reveals no specific changes in the NQA for any tract. (C) The comparison between preop tractography and one-year follow-up shows an unspecific change in the right (threshold 0.50). (D) *Case #2*. Preop tractography vs. immediate postop tractography. No changes in the CTS between both scans are observed. (E) Immediate postop tractography vs. one-year follow-up demonstrates a decrease in the NQA in the right CST. (F) One-year follow-up tractography demonstrates decreased NQA in the right CST, suggesting a compromised function of this tract.

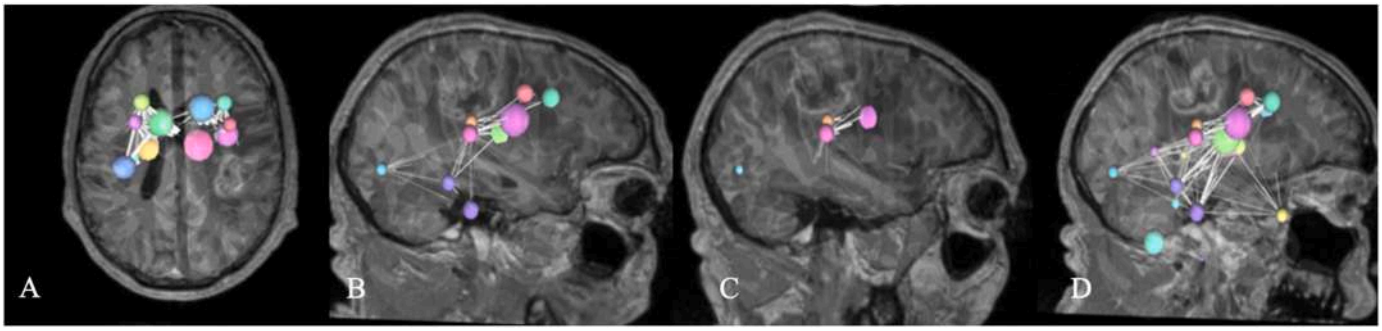

Fig. 6. The control group from the HCP averaged 1200 patients' connectome compared to the T1-enhanced MRI preop images from Case #2. (A) Axial view showing the relationship between normal connectome compared with the tumor architecture. (B-D) Sagittal consecutive slides demonstrate the absence of disruption of the connections by the tumor core and its relationship with the tumor margins.

Hagmann originally introduced the concept of the connectome in 2005 [24]. Connectomics aims to construct a comprehensive map of neuronal connections, not only in healthy conditions but also in pathological settings. The connectivity architecture of whole-brain networks is utilized to model the effective connectivity of an individual.This new perspective is rooted in the concept of the degree of connectivity within a local connectome, which was introduced by Yeh et al. [25]. This concept involves assessing the connectivity between adjacent voxels within a white matter fascicle, which is defined by the density of diffusing spins [25].

This approach provides insights into the local orientation of tracts, including where fibers start and stop, and how they traverse through the core of the white matter. This information is derived from the Human Connectome Project (HCP) [13]. Connectometry analysis utilizes this concept to track segments of the fiber bundle that exhibit significant association with the study variable. This involves reconstructing diffusion MRI data into a standard template based on the baseline space to map a local connectome matrix. This approach offers a comprehensive

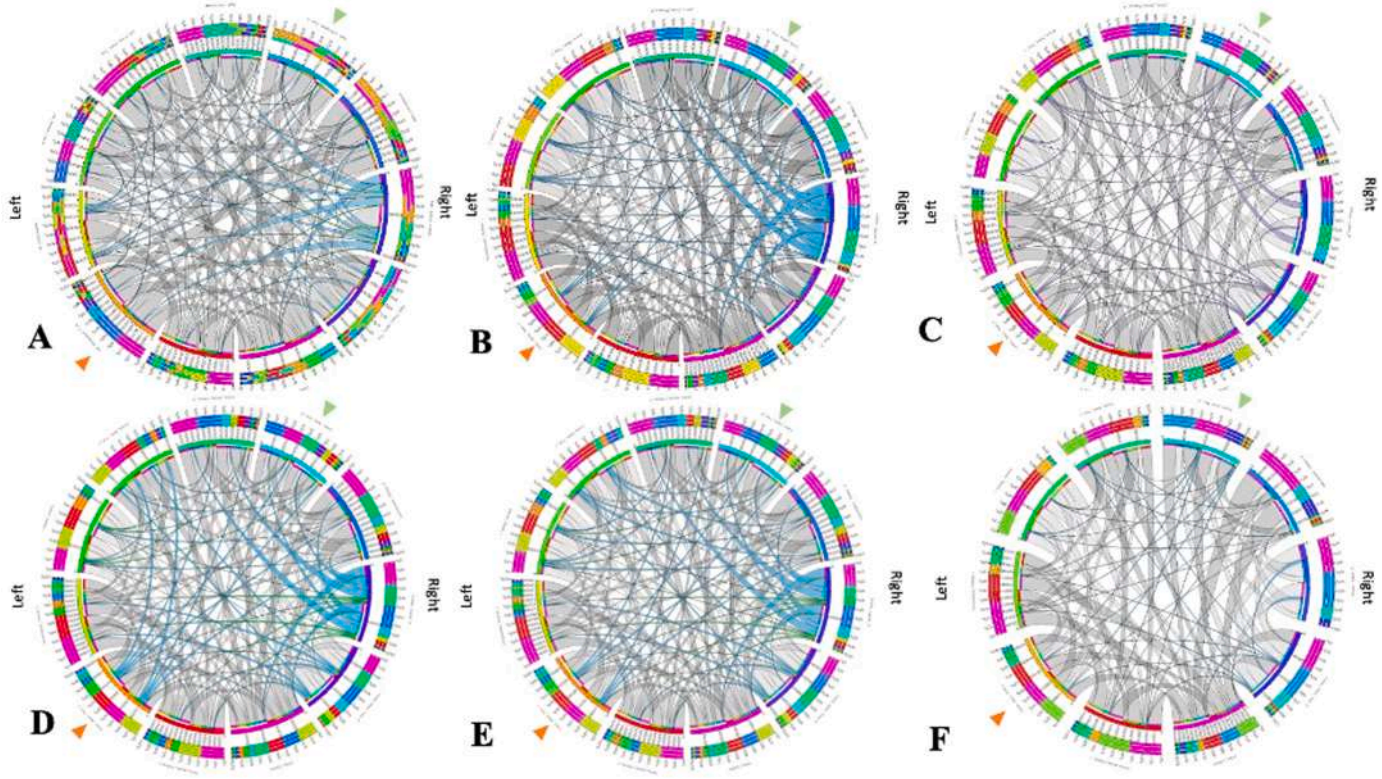

Fig. 7. Connectivity maps of white matter fibers in the preoperative, immediate postoperative, and 1-year follow-up scans. *Green arrowhead*: Right CST, *Orange Arrowhead*: Left CST. *Case #1.* (A) Preoperative connectivity map. White fibers are arranged in a symmetric distribution in both, left and right cortical tracts, noting in blue an increased signal diffusion in the right Aslant tract. (B) Immediate postoperative analysis shows the fiber changes with a tendency for a symmetric distribution and increased signal diffusion in the right-sided tracts. (C) 1-year follow-up connectome shows a similar distribution to the preoperative period, with a symmetric distribution along both hemispheres. However, notice in purple a decreasing signal in the right CST. *Case #2.* (D) Preoperative connectivity map. White fibers are arranged in a symmetric distribution in both, the left and right cortical tracts, note in blue an increased signal diffusion in the right Aslant tract, the left CST, and the right external capsule. (E) Immediate postoperative analysis shows a similar distribution as the preoperative connectogram. (F) 1-year follow-up connectome. At this point, the patient presented with tumoral recurrence, and post-treatment was guided by STUPP protocol. The fibers in this connectogram show a mostly symmetric distribution with a notorious decreased density, compared to previous images, and a persistent decrease on the right, most specifically in the right CST, probably associated with post-treatment changes and tumoral infiltration. The graph was built by quartiles and color-coded for easier interpretation. Q1 interactions, meaning the strongest interaction in the analysis, were selected to appear in light blue, Q2 interactions in green, Q3 light gray, and Q4 in dark grey.

understanding of white matter connectivity and its relation to various clinical variables [26,27].

Fig. 5 illustrates the relationship between the Human Connectome Project (HCP) database and patient tractography, revealing potential additional associations between connections and structural changes induced by the tumor and its environment. Interestingly, the connections were not directly affected by the tumor core but rather by the tumor margin and peritumoral edema, indicating progressive reorganization adapting to the tumor boundaries. This tool allows for a focused analysis of fibers and connections involved, both within and outside the tumor boundaries.

In case #2, we aimed to emphasize how the integrity of connections, compared with 1065 control patients, remains intact despite physical changes in the peritumoral environment, suggesting early brain plasticity. This suggests that despite the presence of the tumor and its effects on surrounding tissue, the brain can adapt and maintain connectivity integrity [28]. One would anticipate either improvements or no changes in NQA and FA values, along with improvements or no changes in clinical outcomes, reflecting the preservation of functional connectivity despite structural changes induced by the tumor.

Our study provides insight into two distinct scenarios: 1) neural reorganization without clinical changes, and 2) neural reorganization accompanied by clinical changes. Further follow-up is necessary to determine whether these findings represent initial radiological indicators preceding clinical improvement or decline in the patient's condition. In this context, DifT may play a potential role in predicting outcomes in motor function. Large sample sizes comparing patients with similar molecular tumor groups could help mitigate bias, given the considerable differences in molecular behavior and natural history of the disease. Our DifT analysis revealed the most significant decrease between the preoperative period and the 1-year follow-up. However, this change is likely associated with tumor recurrence and infiltration of the tract. This underscores the importance of ongoing monitoring and early detection of changes to guide clinical management effectively.

The brain's capacity for neuroplasticity enables it to reorganize by forming new neural connections throughout life. This phenomenon allows the brain to compensate for neoplastic disease and adapt its primary functions accordingly [28]. Studies have demonstrated cortical reorganization in repeat surgeries for recurrent tumors in motor areas using intraoperative cortical stimulation [28,29]. The pattern of neural plasticity and tract reorganization varies individually, influenced by multiple variables such as preoperative neurological compromise, tumor volume, EOR, and molecular profile, among others.

DifT may provide valuable insights into the importance of sequential tractography for investigating postoperative neural reorganization and its relationship with a patient's outcome in the short, medium, and long term. This minimally invasive approach can offer a deeper understanding of a patient's ability to improve with appropriate rehabilitation or deteriorate despite receiving optimal treatment. Ultimately, this information could contribute to personalized treatment strategies and

improved patient care. One could argue that the reduction in connection strength observed in the follow-up imaging for case #2 may be associated with the administration of the STUPP protocol, tumor recurrence, or a combination of both factors. However, there is insufficient data to definitively determine the cause.

This study highlights that the progressive distortion of the brain connectome can be quantified, allowing for individual sequential analyses regarding white matter compromise. Such analyses can provide insights into the association between these changes and the nature of the tumor, as well as how surgical interventions and adjuvant therapies may influence the compromise of the local and whole-brain connectome. This approach could lead to a better understanding of the underlying mechanisms driving changes in brain connectivity following tumor treatment and aid in the development of more targeted and effective therapeutic strategies.

4.1. Limitations of the study

The primary limitation of this study is the small sample size, with only two subjects included, as well as the limited number of follow-up examinations. However, the investigation of the whole connectome in both cases was thorough and comprehensive. Further studies involving more patients, along with additional individual time-spaced diffusion tensor tractography assessments, are necessary to validate our findings.

An inherent limitation of DifT is its inability to provide a comprehensive analysis of track integrity, as it only reflects anisotropy changes within a specific time frame and may yield false-positive results. However, we optimized our results according to recommendations by Yeh et al. [30], employing a high b-value and repeating tests to enhance sensitivity.

Our study sheds light on how the connectome undergoes sequential reorganization in an evolving manner, varying on a case-by-case basis. Nevertheless, a larger sample size would be essential to delineate the key aspects of plasticity definitively. Regarding connectometry, a significant limitation is the unpredictability of fiber rearrangement. As demonstrated in Fig. 7, immediate postoperative changes did not accurately predict whole-brain rearrangement in the follow-up, underscoring the need for mathematical tools to minimize errors and improve the accuracy of predicting recovery. Additionally, in closer follow-ups, these changes may also be associated with early imaging signatures for tumor recurrence, further complicating prediction models.

5. Conclusions

Based on the assessment of NQA, FA values, and changes in tract volume, our findings consistently indicated satisfactory preservation of motor function immediately postoperatively. However, despite the changes observed in the short-term follow-up, both DifT and connectometry/connectogram analyses revealed that reorganization patterns may not necessarily correlate with clinical outcomes in a prospective setting. Instead, these patterns likely reflect the brain's plasticity in response to changes induced by tumor recurrence or adjuvant treatment. Further studies are necessary to corroborate these findings and explore their potential predictive value for prognosis. Understanding how the brain adapts and reorganizes in response to tumor-related changes and therapeutic interventions could lead to improved prognostic tools and treatment strategies for patients with brain tumors.

CRediT authorship contribution statement

Matías Baldoncini: Conceptualization, Funding acquisition, Investigation, Validation, Writing – review & editing. **Fernando Hakim:** Conceptualization, Funding acquisition, Investigation, Supervision, Validation, Writing – review & editing. **Sabino Luzzi:** Conceptualization, Supervision, Validation, Visualization, Writing – review & editing. **Diego Gomez-Amarillo:** Formal analysis, Investigation, Supervision, Validation, Visualization, Writing – review & editing. **Georgi Apostolov:** Conceptualization, Data curation, Validation, Writing – review & editing. **Juan A. Mejía-Cordovez:** Conceptualization, Funding acquisition, Investigation, Methodology, Writing – review & editing. **Polina Angelova:** Conceptualization, Formal analysis, Project administration, Validation, Writing – review & editing. **Luisa F. Figueredo:** Conceptualization, Formal analysis, Investigation, Methodology, Software, Validation, Visualization, Writing – original draft, Writing – review & editing. **Ivo Kehayov:** Data curation, Investigation, Methodology, Validation, Writing – original draft, Writing – review & editing. **Joao P. Almeida:** Conceptualization, Funding acquisition, Investigation, Supervision, Visualization, Writing – original draft, Writing – review & editing. **Edgar G. Ordóñez-Rubiano**: Conceptualization, Data curation, Formal analysis, Investigation, Project administration, Supervision, Validation, Visualization, Writing – original draft, Writing – review & editing. **Herbert D. Pimienta-Redondo:** Writing – original draft, Writing – review & editing, Conceptualization, Formal analysis. **Jason M. Johnson:** Supervision, Validation, Writing – review & editing.

Declaration of Competing Interest

The authors have no conflict of interest to report.

Acknowledgments

None.

References

[1] H.J. Park, K. Friston, Structural and functional brain networks: from connections to cognition, Science 342 (6158) (2013) 1238411, https://doi.org/10.1126/science.1238411.
[2] M. Weller, W. Wick, K. Aldape, et al., Glioma, Nat. Rev. Dis. Prim. 1 (2015) 15017, https://doi.org/10.1038/nrdp.2015.17.
[3] M.S. Berger, G.A. Ojemann, Intraoperative brain mapping techniques in neuro-oncology, Stereotact. Funct. Neurosurg. 58 (1-4) (1992) 153–161, https://doi.org/10.1159/000098989.
[4] F.C. Yeh, I.M. Zaydan, V.R. Suski, et al., Differential tractography as a track-based biomarker for neuronal injury, Neuroimage 202 (2019) 116131, https://doi.org/10.1016/j.neuroimage.2019.116131.
[5] S. Luzzi, R. Galzio, Intraoperative augmented reality fiber tractography for primary motor area glioma resection, World Neurosurg. 180 (2023) 111, https://doi.org/10.1016/j.wneu.2023.09.115.
[6] S. Luzzi, A. Giotta Lucifero, M. Baldoncini, M. Del Maestro, R. Galzio, Postcentral gyrus high-grade glioma: maximal safe anatomic resection guided by augmented reality with fiber tractography and fluorescein, World Neurosurg. 159 (2022) 108, https://doi.org/10.1016/j.wneu.2021.12.072.
[7] S. Luzzi, A. Giotta Lucifero, A. Martinelli, et al., Supratentorial high-grade gliomas: maximal safe anatomical resection guided by augmented reality high-definition fiber tractography and fluorescein, Neurosurg. Focus 51 (2) (2021) E5, https://doi.org/10.3171/2021.5.FOCUS21185.
[8] S. Luzzi, A. Simoncelli, R. Galzio, Impact of augmented reality fiber tractography on the extent of resection and functional outcome of primary motor area tumors, Neurosurg. Focus 56 (1) (2024), https://doi.org/10.3171/2023.10.FOCUS23477.
[9] E.G. Ordonez-Rubiano, J.M. Johnson, N. Abdalá-Vargas, et al., Preoperative tractography algorithm for safe resection of tumors located in the descending motor pathways zone, Surg. Neurol. Int. 14 (2023), https://doi.org/10.25259/SNI_230_2023.
[10] S. Luzzi, A. Giotta Lucifero, Microscope-based augmented reality with diffusion tensor imaging and fluorescein in insular glioma resection, Neurosurg. Focus.: Video 6 (1) (2022) V10, https://doi.org/10.3171/2021.10.FOCVID2157.
[11] W.I. Essayed, F. Zhang, P. Unadkat, G.R. Cosgrove, A.J. Golby, L.J. O'Donnell, White matter tractography for neurosurgical planning: a topography-based review of the current state of the art, Neuroimage Clin. 15 (2017) 659–672, https://doi.org/10.1016/j.nicl.2017.06.011.
[12] C.S. Yu, K.C. Li, Y. Xuan, X.M. Ji, W. Qin, Diffusion tensor tractography in patients with cerebral tumors: a helpful technique for neurosurgical planning and postoperative assessment, Eur. J. Radiol. 56 (2) (2005) 197–204, https://doi.org/10.1016/j.ejrad.2005.04.010.
[13] D.C. Van Essen, S.M. Smith, D.M. Barch, T.E. Behrens, E. Yacoub, K. Ugurbil, The WU-minn human connectome project: an overview, Neuroimage 80 (2013) 62–79, https://doi.org/10.1016/j.neuroimage.2013.05.041.
[14] F.C. Yeh, S. Panesar, D. Fernandes, et al., Population-averaged atlas of the macroscale human structural connectome and its network topology, Neuroimage 178 (2018) 57–68, https://doi.org/10.1016/j.neuroimage.2018.05.027.

[15] D.N. Louis, A. Perry, P. Wesseling, et al., The 2021 WHO classification of tumors of the central nervous system: a summary, Neuro Oncol. 23 (8) (2021) 1231–1251, https://doi.org/10.1093/neuonc/noab106.
[16] G. Reuter, M. Moïse, W. Roll, et al., Conventional and advanced imaging throughout the cycle of care of gliomas, Neurosurg. Rev. (2021) 1–17.
[17] P. Celtikci, D.T. Fernandes-Cabral, F.-C. Yeh, S.S. Panesar, J.C. Fernandez-Miranda, Generalized q-sampling imaging fiber tractography reveals displacement and infiltration of fiber tracts in low-grade gliomas, Neuroradiology 60 (2018) 267–280.
[18] B.C. Brahimaj, R.B. Kochanski, J.J. Pearce, et al., Structural and functional imaging in glioma management, Neurosurgery 88 (2) (2021) 211–221.
[19] R. Kleiser, P. Staempfli, A. Valavanis, P. Boesiger, S. Kollias, Impact of fMRI-guided advanced DTI fiber tracking techniques on their clinical applications in patients with brain tumors, Neuroradiology 52 (2010) 37–46.
[20] F.C. Yeh, A. Irimia, D.C.A. Bastos, A.J. Golby, Tractography methods and findings in brain tumors and traumatic brain injury, Neuroimage 245 (2021) 118651, https://doi.org/10.1016/j.neuroimage.2021.118651.
[21] V.A. Cubon, M. Putukian, C. Boyer, A. Dettwiler, A diffusion tensor imaging study on the white matter skeleton in individuals with sports-related concussion, J. Neurotrauma 28 (2) (2011) 189–201, https://doi.org/10.1089/neu.2010.1430.
[22] F. Henderson Jr., D. Parker, A.A. Vijayakumari, et al., Enhanced fiber tractography using edema correction: application and evaluation in high-grade gliomas, Neurosurgery 89 (2) (2021) 246–256, https://doi.org/10.1093/neuros/nyab129.
[23] P.S. Yen, B.T. Teo, C.H. Chiu, S.C. Chen, T.L. Chiu, C.F. Su, White Matter tract involvement in brain tumors: a diffusion tensor imaging analysis, Surg. Neurol. 72 (5) (2009) 464–469, https://doi.org/10.1016/j.surneu.2009.05.008.
[24] P. Hagmann, L. Cammoun, X. Gigandet, et al., MR connectomics: principles and challenges, J. Neurosci. Methods 194 (1) (2010) 34–45, https://doi.org/10.1016/j.jneumeth.2010.01.014.
[25] F.C. Yeh, T.D. Verstynen, Y. Wang, J.C. Fernández-Miranda, W.Y. Tseng, Deterministic diffusion fiber tracking improved by quantitative anisotropy, PLoS One 8 (11) (2013) e80713, https://doi.org/10.1371/journal.pone.0080713.
[26] F.C. Yeh, Population-based tract-to-region connectome of the human brain and its hierarchical topology, Nat. Commun. 13 (1) (2022) 4933, https://doi.org/10.1038/s41467-022-32595-4.
[27] A. Irimia, M.C. Chambers, C.M. Torgerson, J.D. Van Horn, Circular representation of human cortical networks for subject and population-level connectomic visualization, Neuroimage 60 (2) (2012) 1340–1351, https://doi.org/10.1016/j.neuroimage.2012.01.107.
[28] H. Duffau, L. Taillandier, New concepts in the management of diffuse low-grade glioma: proposal of a multistage and individualized therapeutic approach, Neuro Oncol. 17 (3) (2015) 332–342, https://doi.org/10.1093/neuonc/nou153.
[29] F.C. Yeh, D. Badre, T. Verstynen, Connectometry: a statistical approach harnessing the analytical potential of the local connectome, Neuroimage 125 (2016) 162–171, https://doi.org/10.1016/j.neuroimage.2015.10.053.
[30] F.C. Yeh, V.J. Wedeen, W.Y. Tseng, Generalized q-sampling imaging, IEEE Trans. Med. Imaging 29 (9) (2010) 1626–1635, https://doi.org/10.1109/tmi.2010.2045126.